Molecular Pharmacology Fast Forward. Published on September 24, 2022 as DOI: 10.1124/molpharm.121.000305
This article has not been copyedited and formatted. The final version may differ from this version.

TITLE PAGE

Differential enantiomer-specific signaling of cannabidiol at CB_1 receptors

Taryn Bosquez, Sierra Wilson, Christos Iliopoulos-Tsoutsouvas, Shan Jiang, Jim Wager-Miller, Spyros P. Nikas, Ken P. Mackie, Alexandros Makriyannis, Alex Straiker

TB, SW, JWM, KM, AS: Gill Center for Biomolecular Science, Department of Psychological and Brain Sciences, Program in Neuroscience, Indiana University, Bloomington IN USA 47405
CIT, SPN, AM: Center for Drug Discovery and Department of Pharmaceutical Sciences, Northeastern University, Boston MA USA 02115
SJ, AM: Center for Drug Discovery and Department of Chemistry and Chemical Biology, Northeastern University, Boston MA USA 02115

Molecular Pharmacology Fast Forward. Published on September 24, 2022 as DOI: 10.1124/molpharm.121.000305
This article has not been copyedited and formatted. The final version may differ from this version.

RUNNING TITLE PAGE

Running Title**: CBD enantiomer signaling**

Corresponding authors*:
Alex Straiker
Indiana University
1101 E 10th St.
Bloomington, IN 47405
Tel: 206 850 2400
Email: straiker@indiana.edu

Alexandros Makriyannis
Center for Drug Discovery, Northeastern University
Mugar Life Science Building Rm 116
360 Huntington Avenue
Boston, MA 02115
Tel: 617 373 4200
Email: a.makriyannis@northeastern.edu

* These authors contributed equally

Text pages: 22
Tables: 1
Figures: 5
References: 51
Abstract: 243 words
Introduction: 703 words
Discussion: 1279 words

Key words:
Allosteric, orthosteric, G protein-coupled receptor, cannabinoid receptor, CB1, (+)-CBD, S-CBD

Abbreviations: DSE, depolarization-induced suppression of excitation; 2-AG, 2-arachidonoyl glycerol; NAM, negative allosteric modulator; EPSC, excitatory postsynaptic current; BSA, bovine serum albumin; MTPA, *α*-Methoxy-*α*-(trifluoromethyl)phenylacetyl; CBD, cannabidiol; THC, tetrahydrocannabinol.

Molecular Pharmacology Fast Forward. Published on September 24, 2022 as DOI: 10.1124/molpharm.121.000305
This article has not been copyedited and formatted. The final version may differ from this version.

ABSTRACT

The two main constituents of *Cannabis* are Δ^9-THC and cannabidiol (CBD). While Δ^9-THC pharmacology has been studied extensively, CBD -- long considered inactive -- is now the subject of vigorous research related to epilepsy, pain and inflammation and is popularly embraced as a virtual cure-all. However, our understanding of CBD pharmacology remains limited, though CBD inhibits cannabinoid CB_1 receptor signaling, likely as a negative allosteric modulator. *Cannabis* synthesizes (-)-CBD, but CBD can also exist as an enantiomer, (+)-CBD. We enantioselectively synthesized both CBD enantiomers using established conditions and describe here a new, practical, and reliable, NMR-based method for confirming the enantiomeric purity of two CBD enantiomers. We also investigated the pharmacology of (+)-CBD in autaptic hippocampal neurons, a well-characterized neuronal model of endogenous cannabinoid signaling, and in CHO-K1 cells. We report the Ki for displacing CP55,940 at CB_1 by (+)-CBD, is five-fold lower than (-)-CBD. We find that (+)-CBD is ~10 times more potent at inhibiting depolarization-induced suppression of excitation (DSE), a form of endogenous cannabinoid-mediated retrograde synaptic plasticity. (+)-CBD also inhibits CB_1 suppression of cAMP accumulation but with less potency, indicating that the signaling profiles of the enantiomers differ in a pathway-specific manner. In addition, we report that (+)-CBD stereoselectively and potently activates the sphingosine-1 phosphate (S1P) receptors, $S1P_1$ and $S1P_3$. These results provide an attractive method for synthesizing and distinguishing enantiomers of CBD and related phytocannabinoids and provide further evidence

Molecular Pharmacology Fast Forward. Published on September 24, 2022 as DOI: 10.1124/molpharm.121.000305
This article has not been copyedited and formatted. The final version may differ from this version.

that these enantiomers have their own unique and interesting signaling properties.

SIGNIFICANCE STATEMENT

Cannabidiol (CBD) is the subject of considerable scientific and popular interest, but we know little of the enantiomers of CBD. We find that the enantiomer (+)-CBD is substantially more potent inhibitor of cannabinoid CB_1 receptors and that it activates sphingosine-1-phosphate receptors in an enantiomer-specific manner; we have additionally developed an improved method for the synthesis of enantiomers of CBD and related compounds.

INTRODUCTION

Cannabidiol (CBD) and Δ^9-THC are the phytocannabinoids found in greatest abundance in cannabis (Elsohly and Slade, 2005). CBD was isolated before Δ^9-THC (Adams et al., 1940), but remained poorly studied for decades. Because CBD is non-euphoric and because it competes weakly with conventional orthosteric radioligands for binding at the CB_1 cannabinoid receptor, (Mechoulam et al., 1970; Thomas et al., 1998) CBD was often described as inactive. Yet different ratios of Δ^9-THC and CBD in cannabis preparations yield differential effects (Hiltunen and Jarbe, 1986; Karniol and Carlini, 1973; Petitet et al., 1998; Russo and Guy, 2006) and growers have actively developed cannabis strains with different ratios of CBD and Δ^9-THC satisfying a need of the commercial market. CBD is now an FDA-approved anti-epileptic (reviewed in (O'Connell et

Molecular Pharmacology Fast Forward. Published on September 24, 2022 as DOI: 10.1124/molpharm.121.000305
This article has not been copyedited and formatted. The final version may differ from this version.

al., 2017)) -- though the mechanism is still uncertain -- and shows promise for other potential therapeutic applications (reviewed in (Maccarrone et al., 2017)). As a consequence of this and the rapidly changing cannabis-related legal landscape, there is now a keen interest in how CBD acts in the body.

It is not widely appreciated that CBD can come in more than one form. Many chemical compounds exhibit a 'handedness' and CBD is no exception. Such compounds are structurally identical except that the enantiomers form mirror images of one another, around a chiral center. CBD has two chiral centers and therefore has four potential stereoisomers, giving rise to two pairs of enantiomers. The cannabis plant produces one of these (*R,R*)-CBD -- denoted here as (-)-CBD -- but a series of studies of one enantiomer have reported that the non-natural (*S,S*)-CBD -- here, (+)-CBD -- may have interesting signaling properties. Several studies have reported that the non-natural CBD enantiomer (+)-CBD has a greater binding affinity when compared to its natural counterpart (Bisogno et al., 2001; Fride et al., 2004; Hanus et al., 2005). Leite et al. (Leite et al., 1982) reported that the (+)-CBD and (-)-CBD enantiomers had identical effects in a seizure model but did see a somewhat stronger effect for (+)-CBD in a pentobarbitone sleeping time test. A separate study found the enantiomers to similarly activate the capsaicin receptor TRPV1 and that (+)-CBD inhibits the uptake and subsequent hydrolysis of the endocannabinoid anandamide (AEA) (Bisogno et al., 2001). The (+)-CBD enantiomer has also been reported to possess moderate to potent anti-inflammatory properties that were both

Molecular Pharmacology Fast Forward. Published on September 24, 2022 as DOI: 10.1124/molpharm.121.000305
This article has not been copyedited and formatted. The final version may differ from this version.

dependent and independent of the CB_1 receptor (Fride et al., 2004; Hanus et al., 2005). Those studies were done at a time when it was broadly assumed that CBD was inactive at CB_1 receptors, an assumption grounded in the poor ability of CBD to compete with an orthosteric agonist such as CP55940. Although some hypothesized that CBD interferes with CB_1 activation (Petitet et al., 1998), the mechanism for this was clarified only more recently by evidence for CBD as a negative allosteric modulator of CB_1 (Laprairie et al., 2015). Binding at an allosteric site on CB_1 would account for inhibition of CB_1 signaling despite poor orthosteric binding.

Given our improved understanding of CBD activity at CB_1 receptors, and the keen interest in CBD, now is a suitable time to consider how the enantiomers of CBD act at this receptor. We chose the (+)-CBD enantiomer as a starting point since previous work has focused on this enantiomer. Though the synthesis of CBD enantiomers has been previously described (Hanus et al., 2005), it remains a challenge to prove that each enantiomer, when made, is free from the other enantiomer. This is important in order to evaluate the biological activity of CBD as well as THC analogs. We therefore developed a simple, reliable NMR-based method that can be applied to distinguish between the enantiomers of both CBD and THC. We then tested the signaling properties of (+)-CBD relative to (-)-CBD in two model systems. We have previously shown that (-)-CBD effectively antagonizes CB_1 signaling in a neuronal model of endogenous CB_1- and 2-AG-dependent plasticity (Straiker et al., 2018) and have now similarly examined (+)-CBD. We additionally tested (+)-CBD and (-)-CBD for their effects on both CB_1

Molecular Pharmacology Fast Forward. Published on September 24, 2022 as DOI: 10.1124/molpharm.121.000305
This article has not been copyedited and formatted. The final version may differ from this version.

and sphingosine-1-phosphate (S1P) receptor signaling via the cAMP pathway. We report here that (+)-CBD signaling substantially differs from that of its natural counterpart in a pathway- and target-specific manner.

MATERIALS AND METHODS

Animals and neuronal culture

All animal care and experimental procedures used in this study were approved by the Institutional Animal Care and Use Committee of Indiana University and conform to the Guidelines of the National Institutes of Health on the Care and Use of Animals. Mouse hippocampal neurons isolated from the CA1–CA3 region were cultured on microislands as previously described (Bekkers and Stevens, 1991; Furshpan et al., 1976). Briefly, neurons were obtained from animals (at postnatal day 0–2, killed via rapid decapitation without anesthesia) and plated onto a feeder layer of hippocampal astrocytes that had been laid down previously (Levison and McCarthy, 1991). Cultures were grown in high-glucose (20 mM) minimum essential media containing 10% horse serum, without mitotic inhibitors and used for recordings after 8 days in culture and for no more than 3 h after removal from culture medium (Straiker and Mackie, 2005). All electrophysiological experiments were performed exclusively on excitatory neurons. All tests were made on neurons from at least two different preparations.

Molecular Pharmacology Fast Forward. Published on September 24, 2022 as DOI: 10.1124/molpharm.121.000305
This article has not been copyedited and formatted. The final version may differ from this version.

Electrophysiology

When a single neuron is grown on a small island of permissive substrate, it forms synapses – or 'autapses' – onto itself. All experiments were performed on isolated autaptic neurons. Whole-cell, voltage-clamp recordings from autaptic neurons were carried out at room temperature using an Axopatch 200B amplifier (Molecular Devices, Sunnyvale, CA, USA). The extracellular solution contained (mM) NaCl 119, KCl 5, $CaCl_2$ 2, $MgCl_2$ 1, glucose 30 and HEPES 20. Continuous flow of solution through the bath chamber (~2 $mL \cdot min^{-1}$) ensured rapid drug application and clearance. Drugs were typically prepared as a stock then diluted into extracellular solution at their final concentration and used on the same day. Recording pipettes of 1.8–3 MΩ were filled with solution containing (mM): potassium gluconate 121.5, KCl 17.5, NaCl 9, $MgCl_2$ 1, HEPES 10, EGTA 0.2, MgATP 2 and LiGTP 0.5. Access resistance was monitored and only cells with a stable access resistance were included for data analysis.

Statistical analysis: For electrophysiology analyses, depolarization response curves were obtained to determine inhibition of excitatory synaptic transmission by endogenous 2-AG by depolarizing neurons for progressively longer durations (50 msec, 100 msec, 300 msec, 500 msec, 1 sec, 3 sec and 10 sec). The data were fitted with a nonlinear regression (least squares method, with top of curve (representing no effect) constrained to 1) using GraphPad Prism (La Jolla, CA). This allowed calculation of an ED50, the effective dose or duration of depolarization at which a 50% inhibition is achieved as well as the Emax. Statistically significant differences in these responses were taken as non-

Molecular Pharmacology Fast Forward. Published on September 24, 2022 as DOI: 10.1124/molpharm.121.000305
This article has not been copyedited and formatted. The final version may differ from this version.

overlapping 95% confidence intervals. Nonsignificant differences were determined by overlapping 95% confidence intervals and an alternative analysis of effect size. The alternative analysis was used to avoid mistakenly accepting the null hypothesis of zero difference at the 0.05 level.

Flamindo cAMP assay

Cell culture and transfection: CHO-K1 cells were cultured in high glucose Dulbecco's Modified Eagle Medium/Nutrient Mixture F12 (Ham's Medium) (Thermo Fisher Scientific, Waltham, MA, USA) while HEK293 cells were cultured in high glucose Dulbecco's Modified Eagle Medium (Thermo Fisher Scientific) in each case, media was supplemented with 10% fetal bovine serum and a 1% Pen/Strep solution. Cultures were maintained at 37°C with an atmosphere of 5% CO_2. For the imaging experiments, the cells were dissociated using trypsin-EDTA (0.05%) and cultured on poly-D-lysine pre-coated 18mm glass coverslips in 12-well plates. One day post-plating, the cells were transfected with the receptor of interest (rat CB_1, human $S1P_1$, or human $S1P_3$ receptor), the fluorescent protein EYFP, and the Pink Flamindo cAMP indicator (Harada et al., 2017), using Lipofectamine 2000 Transfection Reagent (Thermo Fisher Scientific). After 3.5 hours, the transfection reagent was replaced with cell culture media and the cells used for experiments within two days of transfection.

Cell imaging and cAMP binding assay: Transfected CHO-K1 or HEK293 cells, were imaged in an extracellular solution containing (mM) NaCl 119, KCl 5, $CaCl_2$

Molecular Pharmacology Fast Forward. Published on September 24, 2022 as DOI: 10.1124/molpharm.121.000305
This article has not been copyedited and formatted. The final version may differ from this version.

2, $MgCl_2$ 1, glucose 30 and HEPES 20, using a Leica TCS SP5 confocal microscope with an oil-immersion 20x objective.

For experiments using CHO-K1 and HEK293 cells, the test compounds were coapplied, followed several minutes later by the adenylyl cyclase activator, forskolin (Fsk; 100μM). Images were acquired every 30 seconds for 15 minutes and then analyzed using FIJI software with the 1-click ROI manager plugin (Thomas and Gehrig, 2020), to measure the change in fluorescence intensity. Target cells were chosen by taking the first image in the series, increasing the brightness, and marking cells that exhibited a baseline Pink Flamindo fluorescence. Occasional (<5%) cells exhibited a high baseline fluorescence relative to the general transfected cell population. These cells were excluded from analysis since they were close to saturation. This mask of identified cells (typically 15-25 per experiment) was then applied to the image series. Baseline fluorescence intensity was normalized to 100 based on the first two minutes of the time series. Using an area under the curve (AUC) analysis for time points from 0 to 15 minutes, administration of a drug concentration series (5nM, 50nM, 100nM, 250nM, and 500nM in CHO-K1-CB_1 cells; 1nM, 10nM, 100nM, 200nM, 500nM, and 1μM in HEK293-wild type cells) allowed the calculation of the IC_{50} for (+)-CBD in this system using Graphpad Prism 6. For a given experimental treatment, a same-day control forskolin-only experimental control was included. Experimental results were compared to their respective same-day controls using an unpaired t-test.

Molecular Pharmacology Fast Forward. Published on September 24, 2022 as DOI: 10.1124/molpharm.121.000305
This article has not been copyedited and formatted. The final version may differ from this version.

Radioligand Binding Assay

Forebrain synaptosomal membranes were prepared from frozen rat brains by the method described by Dodd et al. (Dodd et al., 1981) and were used to assess the affinity for the CB_1 binding sites using [3H]-CP55,940 (specific activity: 81.3 Ci/mmol, NDSP, NIDA) with an excess of unlabeled CP55,940 (30 mM) to determine nonspecific binding. Binding assays were performed at 37°C for 1 hour in the presence of 25 µg protein per well prior to collection of membranes by rapid filtration, washing and scintillation facilitated detection of tritium retained on the membranes as previously described (Janero et al., 2015). The normalized data from three independent experiments were combined and analyzed using a four-parameter logistic equation to yield IC_{50} values that were converted to K_i values using the assumptions of Cheng and Prussoff (Cheng and Prusoff, 1973) (Table 1). NMR spectra were recorded in $CDCl_3$, on a Varian INOVA-500 (^1H at 500 MHz) spectrometer and chemical shifts are reported in units of δ relative to internal TMS.

Materials

Drugs: Baclofen was purchased from Sigma-Aldrich (St. Louis, MO). $S1P_1$/$S1P_3$ dual antagonist VPC23019, and selective $S1P_1$ and $S1P_3$ antagonists, W146 and TY52156 were purchased from Cayman Chemical (Ann Arbor, MI). 10mM stocks of (+)-CBD and (-)-CBD (in ethanol) were stored at -80ºC and diluted

Molecular Pharmacology Fast Forward. Published on September 24, 2022 as DOI: 10.1124/molpharm.121.000305
This article has not been copyedited and formatted. The final version may differ from this version.

shortly before use. Other drugs were initially prepared as a stock in DMSO or ethanol, then diluted using extracellular solution to their final concentration shortly before use.

Chemicals used in synthesis

(*1R,4S*)-*p*-mentha-2,8-dien-1-ol was purchased from AK Scientific, Union City, CA, while (+)-*cis/trans-p*-mentha-2,8-dien-1-ol purchased from Firmenich Inc, Princeton, NJ. All other chemicals and solvents used in the synthesis were purchased from Sigma-Aldrich (St. Louis, MO) and include boron trifluoride diethyl etherate, anhydrous dichloromethane and pyridine, *p*-toluenesulfonic acid monohydrate, olivetol, and *R*-MTPA chloride [(*R*)-3,3,3-trifluoro-2-methoxy-2-phenylpropanoyl chloride].

RESULTS

Enantioselective synthesis and characterization of (+)-CBD and (-)-CBD.

We synthesized both the non-natural (+)-CBD [(*S,S*)-CBD] (**2**) and the natural (-)-CBD [(*R,R*)-CBD] (**4**) enantioselectively (CB_1 K_i values in Table 1), following a general procedure used for the synthesis of CBD analogs (Nikas et al., 2002a; Nikas et al., 2002b; Papahatjis et al., 2002). It involves the condensation of a chiral monoterpenoid alcohol with olivetol in the presence of a catalytic amount of *p*-toluenesulfonic acid. Enantioselective condensation of olivetol (**1**) with (*1R,4S*)-*p*-mentha-2,8-dien-1-ol (purchased from AK Scientific, Union City, CA) produced (+)-CBD (**2**), while with (+)-*cis/trans-p*-mentha-2,8-dien-1-ol (purchased from Firmenich Inc, Princeton, NJ) produced (-)-CBD (**4**) (Fig. 1A) (Nikas et al., 2002a;

Molecular Pharmacology Fast Forward. Published on September 24, 2022 as DOI: 10.1124/molpharm.121.000305
This article has not been copyedited and formatted. The final version may differ from this version.

Nikas et al., 2002b; Papahatjis et al., 2002). It is well-known that (+)-CBD (**2**) is converted to (+)-Δ^8-THC (**3**), after boron trifluoride etherate treatment, and similarly, (-)-CBD (**4**) is converted to (-)-Δ^8-THC (**5**) (Fig. 1A) (Papahatjis et al., 2007; Papahatjis et al., 2002; Papahatjis et al., 2003; Razdan et al., 1974). Therefore, (+)-Δ^8-THC (**3**) and (-)-Δ^8-THC (**5**), derived from (+)-CBD (**2**) and (-)-CBD (**4**) respectively, can be used to indirectly determine the enantiomeric purity of their precursors based on the Mosher ester approach (Dale et al., 1969). Enantiomerically pure (-)-Δ^8-THC (**5**) and (+)-Δ^8-THC (**3**), prepared as reviewed earlier (Thakur et al., 2005) by using enantiomerically pure (-)- and (+)-verbenol (Patent: Makriyannis et al., WO2011/006099A1). Subsequently, enantiomerically pure (-)-Δ^8-THC (**5**) and (+)-Δ^8-THC (**3**), were derivatized with the *R*-MTPA chloride at the phenolic hydroxyl group to afford two diastereomers **6** (S,S,S) and **7** (R, R, S) (Fig. 1B), respectively. Comparison of the ^{1}H-NMR chemical shifts of the methoxy groups of the diastereomeric esters showed a difference between the two diastereomers **6** and **7** (Fig. 1C). This allows the confirmation of the enantiomeric purity of both (+)-Δ^8-THC and (-)-Δ^8-THC. In the current study, we synthesized enantioselectively (+)-CBD (**2**) and we converted it to (+)-Δ^8-THC (**3**) using identical conditions. The (+)-Δ^8-THC (**3**) was then converted to the respective Mosher ester (**6**), using *R*-MTPA chloride. The inspection of the ^{1}H-NMR spectrum of the resulting compound showed no cross-contamination with (-)-Δ^8-THC, reflecting the enantiomeric purity of its precursor, (+)-CBD (**2**). The same procedure was applied for the synthetic (-)-CBD, to confirm that it is devoid of its enantiomer, (+)-CBD.

Molecular Pharmacology Fast Forward. Published on September 24, 2022 as DOI: 10.1124/molpharm.121.000305
This article has not been copyedited and formatted. The final version may differ from this version.

The cannabidiol enantiomer (+)-CBD inhibits neuronal CB_1 signaling more potently than its natural counterpart. We tested whether (+)-CBD would mimic its natural counterpart's ability to suppress synaptic transmission in autaptic hippocampal neurons (Fig. 2). Depolarization of excitatory autaptic hippocampal neurons elicits depolarization induced suppression of excitation (DSE), a form of retrograde synaptic inhibition (Straiker and Mackie, 2005). When neurons are stimulated with a series of successively longer depolarizations (50ms, 100ms, 300ms, 500ms, 1sec, 3 sec, 10 sec) this results in progressively greater inhibition of neurotransmission (Straiker et al., 2011), and yields a "depolarization-response curve". This curve permits the derivation of several pharmacological properties of endogenous cannabinoid signaling, including the calculation of an effective-dose (depolarization) 50 (ED50), the duration of depolarization that results in 50% of the maximal inhibition. A negative allosteric modulator would be expected to shift a depolarization response curve up and to the right (i.e., less DSE in a non-competitive fashion), an effect we previously observed for (-)-CBD (Straiker et al., 2018). We initially tested (+)-CBD at 1μM based on our previous finding that (-)-CBD was fully effective at micromolar concentrations, but soon found that (+)-CBD was more potent than its counterpart. We ultimately tested (+)-CBD at 1nM, 10nM, 100nM, and 1μM finding that 100nM and 1μM CBD fully blocked DSE and that 10nM still substantially inhibited maximal DSE responses (Fig. 3A-B; Baseline Emax (relative EPSC charge (95% CI)): 0.36（0.23-0.48); Emax in presence of 10nM

Molecular Pharmacology Fast Forward. Published on September 24, 2022 as DOI: 10.1124/molpharm.121.000305
This article has not been copyedited and formatted. The final version may differ from this version.

(+)-CBD: 0.72（0.64-0.80); 100nM (+)-CBD: 0.85（0.80-0.89); 1μM (+)-CBD: 0.65（0.49-0.80); 95% CI non-overlapping for 10nM, 100nM and 1μM vs. baseline) with an IC_{50} of 5.5nM (95% CI: 0.4-74). Sample DSE time courses from a single neuron treated with successively higher concentrations of (+)-CBD are shown in Figure 3A. We confirmed our previous finding that 100nM (-)-CBD does not inhibit DSE (Fig. 3C, Baseline DSE in response to 3 sec depolarization (± SEM): 0.62 ± 0.02; DSE with 100nM (-)-CBD (± SEM): 0.58 ± 0.04, n=5, NS by paired t-test). We confirmed that (+)-CBD alone did not inhibit EPSCs and so neither directly inhibits nor activates excitatory neurotransmission in wild-type of CB_1 knockout neurons (Fig. 3D, relative EPSC charge ((+)-CBD 100nM) in WT (± SEM): 1.05 ± 0.04, n=5; in CB_1 KO: 0.99 ± 0.01, n=5).

We also tested whether (+)-CBD interferes with inhibition of EPSCs by bath-applied 2-AG, allowing us to assess whether the effect of (+)-CBD was perhaps due to a post-synaptic alteration of 2-AG release. Using a sub-maximal concentration of 2-AG, 1μM, we found that 100nM (+)-CBD reversed 2-AG effects (Fig. 3E-F, relative EPSC charge 3 minutes after 1uM 2-AG (± SEM): 0.53 ± 0.07; charge relative to original baseline with 2-AG and (+)-CBD (100nM) (± SEM): 0.84 ± 0.07, n=5; $p<0.005$, paired t-test).

To rule out the possibility that the effect of (+)-CBD was due to general inhibition of presynaptic GPCR signaling, we tested for effects on inhibition of EPSCs by an agonist of $GABA_B$, another $G_{i/o}$-coupled receptor that also presynaptically inhibits neurotransmitter release in this neuronal preparation (Straiker et al., 2002). We found that baclofen (25μM) activation of $GABA_B$ still produced the

Molecular Pharmacology Fast Forward. Published on September 24, 2022 as DOI: 10.1124/molpharm.121.000305
This article has not been copyedited and formatted. The final version may differ from this version.

expected inhibition in the presence of 100nM (+)-CBD (Fig. 3G-I, Relative EPSC charge 3 minutes after 25μM baclofen/100nM (+)-CBD (± SEM): 0.40 ± 0.06, n=3; 25μM baclofen only(± SEM): 0.29 ± 0.04, n=3). Figure 3G shows a sample time course of a cell treated with (+)-CBD that had no response to 2-AG (1μM) but a strong, reversible response to baclofen (25μM) while figure 3H shows a separate sample time course for a cell that was treated with baclofen only. Because we found in separate experiments outlined below that (+)-CBD activates S1Px receptors, we tested whether the $S1P_1$/$S1P_3$ receptor antagonist VPC23019 impacts DSE, finding that it does not (Fig. 3J; baseline DSE (± SEM): 0.61 ± 0.02; After VPC23019 (1μM) (± SEM): 0.58 ± 0.04, n=5, NS by paired t-test).

(+)-CBD is a less potent inhibitor of CB_1 receptor cAMP pathway signaling. We additionally tested whether the (+)-CBD enantiomer differentially modulates CB_1-mediated inhibition of cyclic AMP (cAMP) accumulation in CB_1-transfected CHO-K1 cells. As a $G_{i/o}$-coupled GPCR, CB_1 inhibits adenylyl cyclase and as a result disrupts cAMP formation (Howlett et al., 2002). Activity of CB_1 in this pathway is measured as the inhibition of the synthesis of cAMP by adenylyl cyclase. Using Pink Flamindo, a red fluorescent protein-based cAMP indicator (Harada et al., 2017), we measured cAMP accumulation after treatment with the adenylyl cyclase activator, forskolin (Fsk), in a CHO-K1 cell line transfected with the rat CB_1 receptor.

Molecular Pharmacology Fast Forward. Published on September 24, 2022 as DOI: 10.1124/molpharm.121.000305
This article has not been copyedited and formatted. The final version may differ from this version.

We found that both (+)-CBD and (-)-CBD effectively interfered with CB_1-mediated cAMP inhibition by 2-AG (2.5μM, Fig. 4A-B), and that there was no difference between the two enantiomers (IC_{50} for (+)-CBD (95% CI): 150nM (81nM-275nM); (-)-CBD: 290nM (121nM-695nM) overlapping 95% confidence intervals). Using an alternative analysis of effect size, we see only a shift of 178nM (±76nM) from 208nM to 386nM. This difference is modest and is not statistically significant by a t-test (p=0.16, n=3 per condition). (+)-CBD had no effect on cAMP accumulation in the absence of 2-AG (Fig. 4C) or CB_1 (Fig. 5K) in these cells. The differing potency of (+)-CBD for cAMP signaling and suppressing DSE indicates a pathway-dependence of the effects of the enantiomers on CB_1 signaling.

(+)-CBD is a potent agonist at sphingosine-1 phosphate receptors $S1P_1$ and $S1P_3$. In the course of our experiments, we noted that 100nM (+)-CBD inhibited cAMP accumulation in HEK293 cells, even in the absence of CB_1 receptors (Fig. 5A-B; inhibition of Fsk (1.0 = no effect): (+)-CBD: 0.75 ± 0.05; unpaired t-test, p-value< 0.05, (+)-CBD, p=0.007, n=3), while (-)-CBD had no effect even at a higher concentration (1μM). Testing a range of concentrations, we found that the EC_{50} for (+)-CBD was 147nM (Fig. 5C-D; EC_{50} (95% CI): 147nM (47nM-460nM). We hypothesized that (+)-CBD might be acting on a $G_{i/o}$-coupled GPCR endogenously expressed in HEK293 cells. This was confirmed by pretreating cells with pertussis toxin (PTX) overnight, which prevented the effect of (+)-CBD in wild type HEK293 cells (Fig. 5E-G; inhibition of Fsk (1.0 = no effect): (+)-CBD: 0.71 ± 0.04; unpaired t-test, p-value< 0.05, (+)-CBD, p=0.001, n=3).

Molecular Pharmacology Fast Forward. Published on September 24, 2022 as DOI: 10.1124/molpharm.121.000305
This article has not been copyedited and formatted. The final version may differ from this version.

We have previously reported the complement of GPCRs expressed in HEK293 cells (Atwood et al., 2011). This includes several $G_{i/o}$-coupled lipid receptors that have some relationship to cannabinoid receptors, including two sphingosine-1 phosphate receptors, $S1P_1$ and $S1P_3$ (Selley et al., 2013). We therefore tested a dual $S1P_1$/$S1P_3$ antagonist, VPC23019 (10nM-1μM), finding that it blocked the effects of (+)-CBD (100nM) in a concentration dependent manner (Fig. 5H). This indicates that one or both of these S1P receptors accounts for the effects of (+)-CBD. We then tested selective $S1P_1$ and $S1P_3$ antagonists, W146 and TY52156 (each at 100nM), finding that each partially inhibited the effects of (+)-CBD (Fig.5H-J; inhibition of (+)-CBD effect (1.0 = no effect): VPC23019: 0.24 ± 0.08; W146: 0.47 ± 0.07; TY52156: 0.59 ± 0.03; n=3; unpaired t-test, p-value<0.05, VPC23019, p=0.0008; W146, p=0.001; TY52156, p=0.001). This suggested that (+)-CBD activates both receptors to inhibit cAMP accumulation in HEK293 cells.

To explore this further, we transfected CHO-K1 cells with either human $S1P_1$ or $S1P_3$ receptor. We found that (+)-CBD (100nM) reduced cAMP accumulation in each case (Fig. 5L-N; inhibition of (+)-CBD effect (1.0 = no effect) $S1P_1$: 0.62 ± 0.06; $S1P_3$: 0.65 ± 0.05; n=3 for each; unpaired t-test, p-value<0.05, $S1P_1$, p=0.004; $S1P_3$, p=0.002), confirming that (+)-CBD is an agonist at $S1P_1$ and $S1P_3$ receptors. Antagonists W146 (300nM) and TY52156 (300nM) reversed this effect. Each antagonist (VPC23019, W146, and TY52156) was tested alone (1μM) with Fsk to show they did not induce an effect in the absence of (+)-CBD in CHO-$S1P_1$, CHO-$S1P_3$, and wild type HEK293 cells (Fig. 5O-R).

Molecular Pharmacology Fast Forward. Published on September 24, 2022 as DOI: 10.1124/molpharm.121.000305
This article has not been copyedited and formatted. The final version may differ from this version.

DISCUSSION

Cannabis sativa produces Δ^9-THC and CBD as well as numerous additional phytocannabinoids. Most of these phytocannabinoids have chiral centers (Lewis et al., 2017), meaning that one or more additional enantiomers may exist: mirror images with distinct three-dimensional structures and, perhaps, different physiological effects. CBD has two chiral centers, meaning that there are four potential stereoisomers, of which the cannabis plant selectively produces (*R,R*)-CBD denoted here as (-)-CBD. Several studies have examined the (*S,S*)-CBD enantiomer – referred to here as (+)-CBD – but these studies were done at a time when the pharmacology of CBD at CB_1 receptors was still limited and also before CBD was approved as an anticonvulsant. Here we enantioselectively synthesized the two enantiomers and developed a new method to readily distinguish them. Additionally, we have tested the signaling profile of (+)-CBD relative to its natural cousin (-)-CBD. In a neuronal model of endogenous CB_1 signaling, we find that (+)-CBD is an order of magnitude more potent than (-)-CBD. In contrast, the enantiomers have similar potency in the modulation of CB_1 cAMP signaling in CHO-K1 cells, pointing to a pathway-dependence. Interestingly, we were able to determine that (+)-CBD, but not (-)-CBD, activates two members of the cannabinoid-related sphingosine 1 phosphate receptor family, $S1P_1$ and $S1P_3$. This indicates that the signaling profiles of these CBD enantiomers differ substantially, both in terms of signaling pathway and receptor targets.

Molecular Pharmacology Fast Forward. Published on September 24, 2022 as DOI: 10.1124/molpharm.121.000305
This article has not been copyedited and formatted. The final version may differ from this version.

The NMR-based method reported here, is simple, reliable, and less costly, when compared to chiral HPLC approaches, and it has been applied successfully to determine the enantiomeric purity of CBD and THC enantiomers. The method utilizes a key structural feature of the THC molecule termed “phenolic hydroxyl group”. Therefore, there is a high likelihood that this method can also be applied in other chiral terpenoid cannabinoids including cannabis components (e.g., cannabivarin and cannabidivarin, as well as synthetic classical cannabinoids that encompass in their structure the phenolic hydroxyl group.

Because CBD is non-euphoric and competes poorly with cannabinoid receptor ligand binding to cannabinoid receptors (Thomas et al., 1998), the study of CBD pharmacology long lagged behind that of Δ^9-THC. This contributed to an initial and persistent conclusion that CBD was either inactive or that any actions of CBD necessarily occurred via non-cannabinoid receptors, or perhaps even via a receptor-independent mechanism. Prior to the identification of cannabinoid receptors in the early 1990s, CBD enantiomers were employed as a tool to discern whether CBD was likely to act at a receptor or via some other means such as alteration of lipid membrane properties. The rationale was that structurally distinct enantiomers would be expected to have differential effects on receptors. Leite et al., for instance found that (+)-CBD and (-)-CBD had identical anticonvulsive effects on a seizure model and concluded that the effect likely occurred independently of a receptor (Leite et al., 1982). A series of studies

Molecular Pharmacology Fast Forward. Published on September 24, 2022 as DOI: 10.1124/molpharm.121.000305
This article has not been copyedited and formatted. The final version may differ from this version.

tested for enantiomer-specific effects on cannabinoid-related targets such as endocannabinoid uptake or TRPV1 receptors (Bisogno et al., 2001), and for orthosteric binding at CB_1 (Fride et al., 2004; Hanus et al., 2005). The latter reported that (+)-CBD binds more potently at the orthosteric site than (-)-CBD, a finding that we have confirmed here.

The last half-dozen years have seen a dramatic reappraisal of the role and mechanism of action for CBD. There is growing evidence that CBD acts via non-canonical cannabinoid-related receptors such as GPR55 (Pertwee, 2008; Senn et al., 2020) and also evidence that CBD acts on CB_1 receptors despite its poor competition with CB_1 orthosteric ligands (Thomas et al., 2007). The likely explanation is that CBD is a negative allosteric modulator at CB_1 (Laprairie et al., 2015). CBD therefore *does* bind to CB_1 but at a secondary allosteric site that escapes observation during CP55940-based equilibrium binding assays. We therefore revisited the activity of (+)-CBD in several assays of CB_1 signaling. We had previously tested the activity of (-)-CBD (Straiker et al., 2018) in excitatory autaptic hippocampal neurons, a well-characterized model of CB_1-mediated plasticity. An architecturally simple system wherein a single neuron synapses onto itself, autaptic neurons express DSE, a 2-AG- and CB_1-mediated form of retrograde inhibition (Straiker and Mackie, 2005). (+)-CBD proved to be 10x more potent than its cousin in this model, but (+)-CBD showed little difference in inhibiting cAMP signaling, an indicator of substantial pathway-specific differences in the signaling of these enantiomers. In principle, it is possible that the difference

Molecular Pharmacology Fast Forward. Published on September 24, 2022 as DOI: 10.1124/molpharm.121.000305
This article has not been copyedited and formatted. The final version may differ from this version.

in (+)-CBD potency between our DSE and cAMP signaling models is due to the difference between the mouse (for DSE experiments) and rat (for cAMP experiments); we have previously reported on species differences in CB_1 signaling for human vs. rat in the autaptic model (Straiker et al., 2012). However, there is only a single amino acid difference between mouse and rat CB1 receptors and this residue is not in a conserved region and has not been otherwise implicated in differential signaling between mouse and rat. Nor have we noted differences in CB1 responses in autaptic cultures derived from rat (Straiker et al., 2002) vs. mouse (Straiker and Mackie, 2005). We therefore consider it unlikely that a species difference between mouse and rat underlies the difference in (+)-CBD potency seen here.

Previous work has shown both the natural and non-natural CBD enantiomers may target a variety of receptors and channels (Bisogno et al., 2001; Fride et al., 2004; Hanus et al., 2005). We report here that unlike (-)-CBD, (+)-CBD activates the S1P receptor subtypes, $S1P_1$ and $S1P_3$ with an EC_{50} of ~150nM. The S1P GPCR family consists of five subtypes $S1P_{1-5}$, receptors that, with the exception of $S1P_4$, are expressed throughout the CNS (Choi and Chun, 2013; Dusaban et al., 2017; Grassi et al., 2019; Lucaciu et al., 2020). With their varying degrees of expression and function in glial cell-types and neurons, $S1P_1$ and $S1P_3$ are implicated in neurogenesis in the developing rodent brain (Choi and Chun, 2013; Ye et al., 2016), blood brain barrier integrity (Groves et al., 2013; Spampinato et al., 2015), stress resilience (Corbett et al., 2019), neuropathic pain (Chen et al.,

Molecular Pharmacology Fast Forward. Published on September 24, 2022 as DOI: 10.1124/molpharm.121.000305
This article has not been copyedited and formatted. The final version may differ from this version.

2019), as well inflammation (Corbett et al., 2019; Dusaban et al., 2017; Spampinato et al., 2015). This has made them targets for the treatment of neurological disorders such as multiple sclerosis, Alzheimer's, Parkinson's, and Huntington's disease (Choi and Chun, 2013; Grassi et al., 2019; Groves et al., 2013; Lucaciu et al., 2020). (+)-CBD may activate other members of this receptor family but determining this would be outside the scope of the current study. Though we hypothesize that the greater potency of (+)-CBD in our autaptic model, is due to allosteric effects on DSE. Though we did not see an effect of (+)-CBD on EPSCs in CB_1 knockout neurons and we found the $S1P_1/_3$ antagonist VPC23019 to be without effect on DSE, it remains possible that the effects of (+)-CBD on DSE occur through some non-CB_1-dependent action.

In summary, we have examined the signaling of (+)-CBD, an enantiomer of the phytocannabinoid CBD that is not produced by the cannabis plant. We find that the signaling of the (+)-CBD enantiomer differs from its cousin in a pathway- and target-dependent manner. In a neuronal model of CB_1-dependent inhibition of neurotransmission, (+)-CBD proved much more potent, when compared to its effect on cAMP accumulation, relative to (-)-CBD. In addition, the (+)-CBD enantiomer was also found to activate the lipid receptors $S1P_1$ and $S1P_3$, which warrants further exploration into whether (+)-CBD could be used to treat or mitigate the severity of various neurological disorders. The finding that the non-natural enantiomer is a much more potent inhibitor of CB_1-dependent neuronal

Molecular Pharmacology Fast Forward. Published on September 24, 2022 as DOI: 10.1124/molpharm.121.000305
This article has not been copyedited and formatted. The final version may differ from this version.

signaling is also noteworthy, given the therapeutic promise and widespread public use of CBD and suggests that enantiomer-specific effects of phytocannabinoids may merit further consideration and experimentation.

ACKNOWLEDGEMENTS

Research was supported by National Institute of Heath grants DA009158 (KM, AM), DA041435 (AM), DA045020 (AM), as well as an Indiana University Grand Challenges grant (AS). Imaging of the Flamindo-based cAMP sensor was made possible by the Indiana University Light Microscopy Imaging Center (LMIC).

AUTHORHSIP CONTRIBUTIONS:

Participated in research design: Bosquez, Wilson, Nikas, Makriyannis, Straiker, and Mackie.

Conducted experiments: Bosquez, Wilson, Jiang, Nikas, and Straiker.

Contributed new reagents or analytic tools: Iliopoulos-Tsoutsouvas, Jiang, Wager-Miller, Nikas, Makriyannis, Straiker, and Mackie.

Performed data analysis: Bosquez, Wilson, Nikas, and Straiker.

Wrote or contributed to the writing of the manuscript: Bosquez, Wilson, Iliopoulos-Tsoutsouvas, Nikas, Makriyannis, Straiker, and Mackie.

Molecular Pharmacology Fast Forward. Published on September 24, 2022 as DOI: 10.1124/molpharm.121.000305
This article has not been copyedited and formatted. The final version may differ from this version.

REFERENCES

Adams R, Hunt M and Clark JH (1940) Structure of cannabidiol, a product isolated from the marihuana extract of Minnesota wild hemp. *Journal of the American Chemical Society* **62**: 4.

Atwood BK, Lopez J, Wager-Miller J, Mackie K and Straiker A (2011) Expression of G protein-coupled receptors and related proteins in HEK293, AtT20, BV2, and N18 cell lines as revealed by microarray analysis. *BMC Genomics* **12**: 14.

Bekkers JM and Stevens CF (1991) Excitatory and inhibitory autaptic currents in isolated hippocampal neurons maintained in cell culture. *Proc Natl Acad Sci U S A* **88**(17): 7834-7838.

Bisogno T, Hanus L, De Petrocellis L, Tchilibon S, Ponde DE, Brandi I, Moriello AS, Davis JB, Mechoulam R and Di Marzo V (2001) Molecular targets for cannabidiol and its synthetic analogues: effect on vanilloid VR1 receptors and on the cellular uptake and enzymatic hydrolysis of anandamide. *Br J Pharmacol* **134**(4): 845-852.

Chen Z, Doyle TM, Luongo L, Largent-Milnes TM, Giancotti LA, Kolar G, Squillace S, Boccella S, Walker JK, Pendleton A, Spiegel S, Neumann WL, Vanderah TW and Salvemini D (2019) Sphingosine-1-phosphate receptor 1 activation in astrocytes contributes to neuropathic pain. *Proc Natl Acad Sci U S A* **116**(21): 10557-10562.

Cheng Y and Prusoff WH (1973) Relationship between the inhibition constant (K1) and the concentration of inhibitor which causes 50 per cent inhibition (I50) of an enzymatic reaction. *Biochem Pharmacol* **22**(23): 3099-3108.

Choi JW and Chun J (2013) Lysophospholipids and their receptors in the central nervous system. *Biochim Biophys Acta* **1831**(1): 20-32.

Corbett BF, Luz S, Arner J, Pearson-Leary J, Sengupta A, Taylor D, Gehrman P, Ross R and Bhatnagar S (2019) Sphingosine-1-phosphate receptor 3 in the medial prefrontal cortex promotes stress resilience by reducing inflammatory processes. *Nature communications* **10**(1): 3146.

Dale JA, Dull DL and Mosher HS (1969) α-Methoxy-α-trifluoromethylphenylacetic acid, a versatile reagent for the determination of enantiomeric composition of alcohols and amines. *J Org Chem* **34**(9): 7.

Dodd PR, Hardy JA, Oakley AE, Edwardson JA, Perry EK and Delaunoy JP (1981) A rapid method for preparing synaptosomes: comparison, with alternative procedures. *Brain Res* **226**(1-2): 107-118.

Dusaban SS, Chun J, Rosen H, Purcell NH and Brown JH (2017) Sphingosine 1-phosphate receptor 3 and RhoA signaling mediate inflammatory gene expression in astrocytes. *J Neuroinflammation* **14**(1): 111.

Elsohly MA and Slade D (2005) Chemical constituents of marijuana: the complex mixture of natural cannabinoids. *Life Sci* **78**(5): 539-548.

Fride E, Feigin C, Ponde DE, Breuer A, Hanus L, Arshavsky N and Mechoulam R (2004) (+)-Cannabidiol analogues which bind cannabinoid receptors but exert peripheral activity only. *Eur J Pharmacol* **506**(2): 179-188.

Furshpan EJ, MacLeish PR, O'Lague PH and Potter DD (1976) Chemical transmission between rat sympathetic neurons and cardiac myocytes developing in microcultures: evidence for cholinergic, adrenergic, and dual-function neurons. *Proc Natl Acad Sci U S A* **73**(11): 4225-4229.

Grassi S, Mauri L, Prioni S, Cabitta L, Sonnino S, Prinetti A and Giussani P (2019) Sphingosine 1-Phosphate Receptors and Metabolic Enzymes as Druggable Targets for Brain Diseases. *Front Pharmacol* **10**: 807.

Groves A, Kihara Y and Chun J (2013) Fingolimod: direct CNS effects of sphingosine 1-phosphate (S1P) receptor modulation and implications in multiple sclerosis therapy. *J Neurol Sci* **328**(1-2): 9-18.

Hanus LO, Tchilibon S, Ponde DE, Breuer A, Fride E and Mechoulam R (2005) Enantiomeric cannabidiol derivatives: synthesis and binding to cannabinoid receptors. *Org Biomol Chem* **3**(6): 1116-1123.

Harada K, Ito M, Wang X, Tanaka M, Wongso D, Konno A, Hirai H, Hirase H, Tsuboi T and Kitaguchi T (2017) Red fluorescent protein-based cAMP indicator applicable to optogenetics and in vivo imaging. *Sci Rep* **7**(1): 7351.

Hiltunen AJ and Jarbe TU (1986) Cannabidiol attenuates delta 9-tetrahydrocannabinol-like discriminative stimulus effects of cannabinol. *Eur J Pharmacol* **125**(2): 301-304.

Howlett AC, Barth F, Bonner TI, Cabral G, Casellas P, Devane WA, Felder CC, Herkenham M, Mackie K, Martin BR, Mechoulam R and Pertwee RG (2002) International Union of Pharmacology. XXVII. Classification of cannabinoid receptors. *Pharmacol Rev* **54**(2): 161-202.

Janero DR, Yaddanapudi S, Zvonok N, Subramanian KV, Shukla VG, Stahl E, Zhou L, Hurst D, Wager-Miller J, Bohn LM, Reggio PH, Mackie K and Makriyannis A (2015) Molecular-interaction and signaling profiles of AM3677, a novel covalent agonist selective for the cannabinoid 1 receptor. *ACS chemical neuroscience* **6**(8): 1400-1410.

Karniol IG and Carlini EA (1973) Pharmacological interaction between cannabidiol and delta 9-tetrahydrocannabinol. *Psychopharmacologia* **33**(1): 53-70.

Laprairie RB, Bagher AM, Kelly ME and Denovan-Wright EM (2015) Cannabidiol is a negative allosteric modulator of the cannabinoid CB1 receptor. *Br J Pharmacol* **172**(20): 4790-4805.

Leite JR, Carlini EA, Lander N and Mechoulam R (1982) Anticonvulsant effects of the (-) and (+)isomers of cannabidiol and their dimethylheptyl homologs. *Pharmacology* **24**(3): 141-146.

Levison SW and McCarthy KD (1991) Characterization and partial purification of AIM: a plasma protein that induces rat cerebral type 2 astroglia from bipotential glial progenitors. *J Neurochem* **57**(3): 782-794.

Lewis MM, Yang Y, Wasilewski E, Clarke HA and Kotra LP (2017) Chemical Profiling of Medical Cannabis Extracts. *ACS Omega* **2**(9): 6091-6103.

Lucaciu A, Brunkhorst R, Pfeilschifter JM, Pfeilschifter W and Subburayalu J (2020) The S1P-S1PR Axis in Neurological Disorders-Insights into Current and Future Therapeutic Perspectives. *Cells* **9**(6).

Maccarrone M, Maldonado R, Casas M, Henze T and Centonze D (2017) Cannabinoids therapeutic use: what is our current understanding following the introduction of THC, THC:CBD oromucosal spray and others? *Expert Rev Clin Pharmacol* **10**(4): 443-455.

Mechoulam R, Shani A, Edery H and Grunfeld Y (1970) Chemical basis of hashish activity. *Science* **169**(3945): 611-612.

Nikas SP, Thakur G and Makriyannis A (2002a) Regiospecifically deuterated (-)-D9-tetrahydrocannabivarins. *J Chem Soc Perkin Trans* **1**: 5.

Nikas SP, Thakur G and Makriyannis A (2002b) Synthesis of side chain specifically deuterated (-)-D9-tetrahydroxycannabinols. *J Labelled Compd Radiopharm* **45**: 12.

O'Connell BK, Gloss D and Devinsky O (2017) Cannabinoids in treatment-resistant epilepsy: A review. *Epilepsy Behav*.

Papahatjis DP, Nahmias VR, Nikas SP, Andreou T, Alapafuja SO, Tsotinis A, Guo J, Fan P and Makriyannis A (2007) C1'-cycloalkyl side chain pharmacophore in tetrahydrocannabinols. *J Med Chem* **50**(17): 4048-4060.

Papahatjis DP, Nikas SP, Andreou T and Makriyannis A (2002) Novel 1',1'-chain substituted Delta(8)-tetrahydrocannabinols. *Bioorg Med Chem Lett* **12**(24): 3583-3586.

Papahatjis DP, Nikas SP, Kourouli T, Chari R, Xu W, Pertwee RG and Makriyannis A (2003) Pharmacophoric requirements for the cannabinoid side chain. Probing the cannabinoid receptor subsite at C1'. *J Med Chem* **46**(15): 3221-3229.

Pertwee RG (2008) The diverse CB1 and CB2 receptor pharmacology of three plant cannabinoids: delta9-tetrahydrocannabinol, cannabidiol and delta9-tetrahydrocannabivarin. *Br J Pharmacol* **153**(2): 199-215.

Petitet F, Jeantaud B, Reibaud M, Imperato A and Dubroeucq MC (1998) Complex pharmacology of natural cannabinoids: evidence for partial agonist activity of delta9-tetrahydrocannabinol and antagonist activity of cannabidiol on rat brain cannabinoid receptors. *Life Sci* **63**(1): PL1-6.

Razdan RK, Dalzell HC and Handrick GR (1974) Hashish. A simple one-step synthesis of (-)-delta1-tetrahydrocannabinol (THC) from p-mentha-2,8-dien-1-ol and olivetol. *J Am Chem Soc* **96**(18): 5860-5865.

Russo E and Guy GW (2006) A tale of two cannabinoids: the therapeutic rationale for combining tetrahydrocannabinol and cannabidiol. *Med Hypotheses* **66**(2): 234-246.

Selley DE, Welch SP and Sim-Selley LJ (2013) Sphingosine lysolipids in the CNS: endogenous cannabinoid antagonists or a parallel pain modulatory system? *Life Sci* **93**(5-6): 187-193.

Senn L, Cannazza G and Biagini G (2020) Receptors and Channels Possibly Mediating the Effects of Phytocannabinoids on Seizures and Epilepsy. *Pharmaceuticals (Basel)* **13**(8).

Spampinato SF, Obermeier B, Cotleur A, Love A, Takeshita Y, Sano Y, Kanda T and Ransohoff RM (2015) Sphingosine 1 Phosphate at the Blood Brain Barrier: Can the Modulation of S1P Receptor 1 Influence the Response of Endothelial Cells and Astrocytes to Inflammatory Stimuli? *PLoS ONE* **10**(7): e0133392.

Straiker A, Dvorakova M, Zimmowitch A and Mackie K (2018) Cannabidiol Inhibits Endocannabinoid Signaling in Autaptic Hippocampal Neurons. *Mol Pharmacol* **94**(1): 743-748.

Straiker A and Mackie K (2005) Depolarization-induced suppression of excitation in murine autaptic hippocampal neurones. *J Physiol* **569**(Pt 2): 501-517.

Straiker A, Wager-Miller J, Hutchens J and Mackie K (2011) Differential signaling in human cannabinoid CB(1) receptors and their splice variants in autaptic hippocampal neurons. *Br J Pharmacol*.

Straiker A, Wager-Miller J, Hutchens J and Mackie K (2012) Differential signalling in human cannabinoid CB1 receptors and their splice variants in autaptic hippocampal neurones. *Br J Pharmacol* **165**(8): 2660-2671.

Straiker AJ, Borden CR and Sullivan JM (2002) G-Protein alpha Subunit Isoforms Couple Differentially to Receptors that Mediate Presynaptic Inhibition at Rat Hippocampal Synapses. *J Neurosci* **22**(7): 2460-2468.

Thakur G, Nikas SP, Duclos R and Makriyannis A (2005) Synthetic methods for cannabinergic ligands., in *Marijuana and cannabinoid research: Methods and protocols* (Onaivi ES ed) pp 113-148, Humana Press Inc.

Thomas A, Baillie GL, Phillips AM, Razdan RK, Ross RA and Pertwee RG (2007) Cannabidiol displays unexpectedly high potency as an antagonist of CB(1) and CB(2) receptor agonists in vitro. *Br J Pharmacol*.

Thomas BF, Gilliam AF, Burch DF, Roche MJ and Seltzman HH (1998) Comparative receptor binding analyses of cannabinoid agonists and antagonists. *J Pharmacol Exp Ther* **285**(1): 285-292.

Ye Y, Zhao Z, Xu H, Zhang X, Su X, Yang Y, Yu X and He X (2016) Activation of Sphingosine 1-Phosphate Receptor 1 Enhances Hippocampus Neurogenesis in a Rat Model of Traumatic Brain Injury: An Involvement of MEK/Erk Signaling Pathway. *Neural plasticity* **2016**: 8072156.

FOOTNOTES

Molecular Pharmacology Fast Forward. Published on September 24, 2022 as DOI: 10.1124/molpharm.121.000305
This article has not been copyedited and formatted. The final version may differ from this version.

I certify that any affiliations with or involvement (either competitive or amiable) in any organization or entity with a direct financial interest in the subject matter or materials discussed in the manuscript (e.g., employment, consultancies, stock ownership, honoraria, expert testimony, etc.) are noted below. All financial research or project support is identified in an acknowledgment in the manuscript Statement of Financial Interest. No author has an actual or perceived conflict of interest with the contents of this article.

This work was supported by the National Institutes of Health National Institute on Drug Abuse [Grants DA009158, DA0141435, and DA045020].

Molecular Pharmacology Fast Forward. Published on September 24, 2022 as DOI: 10.1124/molpharm.121.000305
This article has not been copyedited and formatted. The final version may differ from this version.

LEGENDS FOR FIGURES

Figure 1. Enantioselective synthesis and characterization of (+)-CBD and (-)-CBD. A) Enantioselective synthesis of (+)-CBD and (-)-CBD and their transformation to (+)-Δ^8-THC and (-)-Δ^8-THC respectively. B) Mosher ester derivatization of (+)-Δ^8-THC and (-)-Δ^8-THC. C) ^{1}H-NMR shift of the methoxy protons of the two diastereomeric Mosher esters.

Figure 2. Schematic of DSE in autaptic hippocampal neurons. A) Diagram of neuronal synapse (presynapse above) shows the steps in depolarization-induced suppression of excitation (DSE). Post-synaptic depolarization (lightning bolt) activates diacylglycerol lipase (DAGL) which converts PIP2 to 2-AG. 2-AG crosses the synapse to act on presynaptic CB_1 receptors and is subsequently metabolized by monoacyl glycerol lipase (MAGL). CB_1 activation inhibits calcium channel activation, reducing glutamate release in response to an action potential (black curved arrow). The net effect is a reduction in postsynaptic AMPA receptor activation. B) Upper panels show solitary autaptic neurons in brightfield (with attached recording pipette) and after cell filling. Lower panel shows postsynaptic currents before (green), after inhibition from depolarization (red). C) Schematic representation of DSE shows PSCs that are repeatedly elicited by 1ms depolarization. These are inhibited for tens of seconds after a 3 second DSE stimulus. D) Sample time series showing EPSC responses to increasing durations of depolarization (50ms to 10 sec). E) Depolarization-response curve showing increased inhibition in response to longer durations of depolarization (1.0 = no effect). DSE is absent in CB1 knockout cultures.

Figure 3. (+)-Cannabidiol ((+)-CBD) suppresses CB_1 receptor-mediated depolarization induced suppression of excitation (DSE). A) Sample DSE responses show that 10nM but not 1nM (+)-CBD treatment (5 mins) inhibits CB1-mediated DSE. B) (+)-CBD shifts the response curve for depolarization induced suppression of excitation (DSE) in a concentration-dependent manner. C) At 100nM, (+)-CBD substantially inhibits DSE whereas (-)-CBD does not. D) (+)-CBD (100nM) does not directly inhibit excitatory post-synaptic currents. E) Representative time course shows that 2-AG responses (1μM) are reversed 100nM (+)-CBD. F) Summary results for D. G) Sample experiment showing that $GABA_B$ responses (25μM baclofen) are unaltered by 100nM (+)-CBD treatment. H) Sample control time course for baclofen. I) Summary of results for G-H. Error bars indicate SEM. J) $S1P_{1/3}$ antagonist VPC23019 does not affect DSE. *, $p<0.05$ by paired t-test.

Figure 4. (+)-CBD suppresses CB_1 receptor-mediated cAMP inhibition in CHO-K1 cells. A) Sample time courses in CB_1 transfected CHO-K1 cells show that (+)-CBD concentration-dependently reverses 2AG-induced cAMP inhibition. B) Summarized data from multiple experiments (n=3) and AUC analysis reveal IC_{50}'s for the enantiomers ((+)-CBD (95%CI): 150nM (81nM-275nM); (-)-CBD:

Molecular Pharmacology Fast Forward. Published on September 24, 2022 as DOI: 10.1124/molpharm.121.000305
This article has not been copyedited and formatted. The final version may differ from this version.

290nM (121nM-695nM). C) Sample time courses with CB_1 transfected CHO-K1 cells show (+)-CBD has no effect on CB_1 signaling in the absence of a CB_1 agonist. D) Summary of (+)-CBD signaling in CB_1-transfected CHO-K1 cells using AUC analysis.

Figure 5. (+)-CBD but not (-)-CBD is an agonist at sphingosine 1 phosphate receptors. A) Sample time courses in wild type HEK293 cells show that (+)-CBD but not (-)-CBD reduces forskolin-induced rises in cAMP. B) Summary of (x)-CBD signaling in wild type HEK293 cells using AUC analysis. C) Sample concentration-response time courses for (+)-CBD in wild type HEK293 cells. D) Summarized data from multiple experiments (EC_{50} (95%CI): 147nM (47nM-460nM)). E) Sample time course showing (+)-CBD effect in wild type HEK293 cells. F) Sample time course showing (+)-CBD effect is abolished following pertussis toxin (PTX) treatment in wild type HEK293 cells. G) Summary of (+)-CBD signaling in both non-PTX and PTX treated wild type HEK293 cells using AUC analysis. H) Sample time courses showing the concentration-response for the dual $S1P_1$/$S1P_3$ blocker VPC23019 in wild type HEK293 cells. I) Sample time courses show the effect of (+)-CBD is partly blocked by the $S1P_1$ blocker W146 (100nM) or the $S1P_3$ blocker TY52156 (100nM) and almost fully blocked by the dual $S1P_{1/3}$ blocker VPC23019 (100nM) in wild type HEK293 cells. J) Summary of data with S1Px blockers using AUC analysis. K) Sample time courses show (+)-CBD had no effect in wild type CHO-K1 cells. L) Sample time course shows the effect of (+)-CBD in $S1P_1$-transfected CHO-K1 cells and its inhibition by $S1P_1$ antagonist, W146. M) Sample time course shows the effect of (+)-CBD in $S1P_3$-transfected CHO-K1 cells and its inhibition by $S1P_3$ antagonist, TY52156. N) Summary of (+)-CBD signaling in CHO-K1 cells using AUC analysis. O) Sample time course shows $S1P_1$ antagonist, W146, has no effect on forskolin-induced cAMP signaling in $S1P_1$-transfected CHO-K1 cells. P) Sample time course shows $S1P_3$ antagonist, TY52156, has no effect on forskolin-induced cAMP signaling in $S1P_3$-transfected CHO-K1 cells. Q) Sample time course shows dual $S1P_{1/3}$ blocker, VPC23019, has no effect on forskolin-induced cAMP signaling in wild type HEK293 cells. R) Summary of $S1P_x$ antagonist signaling in CHO-K1 and HEK293 cells using AUC analysis. *, $p<0.05$ by an unpaired t-test vs. 1 (no effect). n=3 for all experiments.

TABLES

Table 1

Compound	CB_1 binding affinity (K_i)
(-)-CBD	1265* nM
(+)-CBD	255 nM

*, (Papahatjis et al., 2002)

Figure 1

Molecular Pharmacology Fast Forward. Published on September 24, 2022 as DOI: 10.1124/molpharm.121.000305
This article has not been copyedited and formatted. The final version may differ from this version.

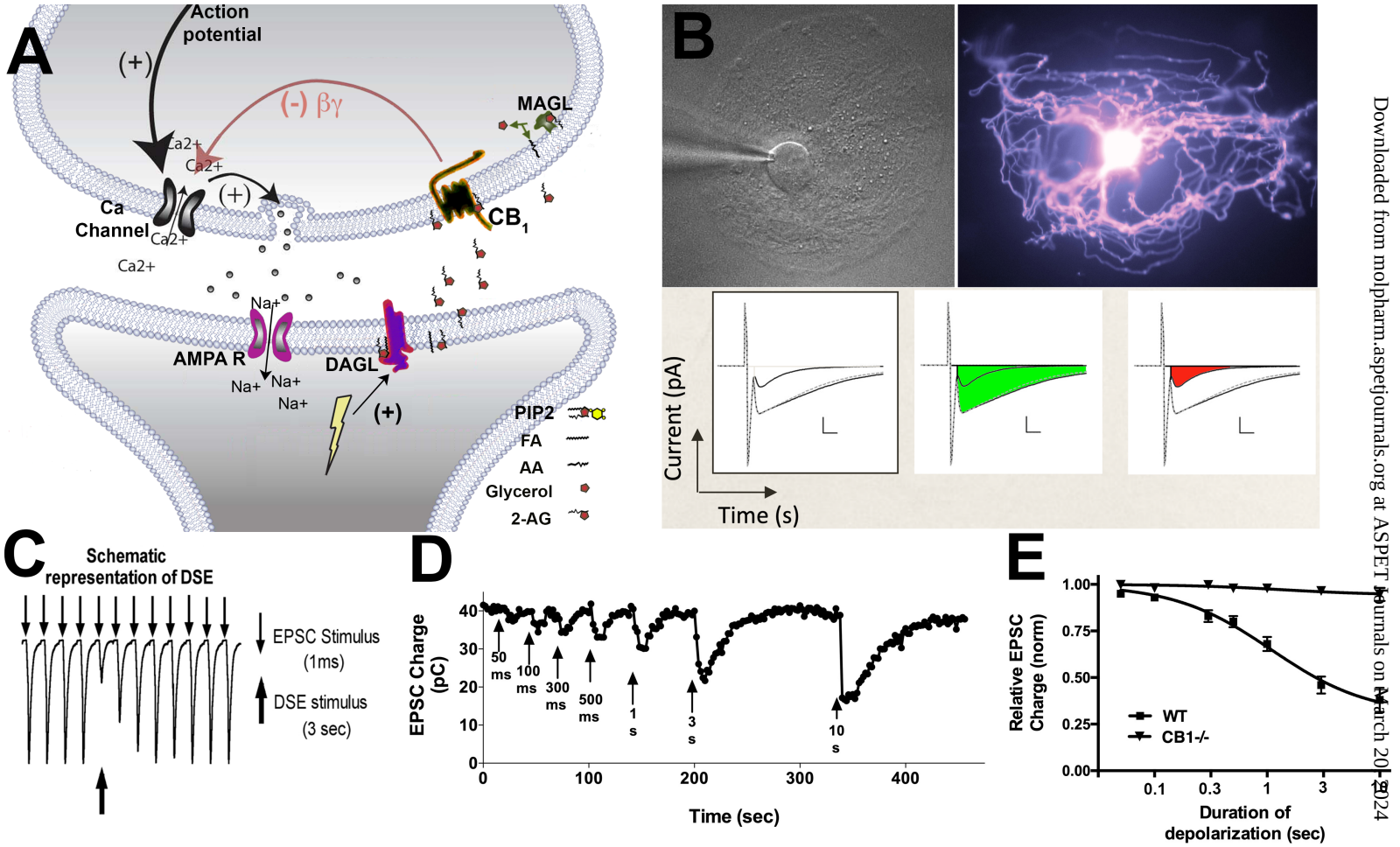

Figure 2

Molecular Pharmacology Fast Forward. Published on September 24, 2022 as DOI: 10.1124/molpharm.121.000305
This article has not been copyedited and formatted. The final version may differ from this version.

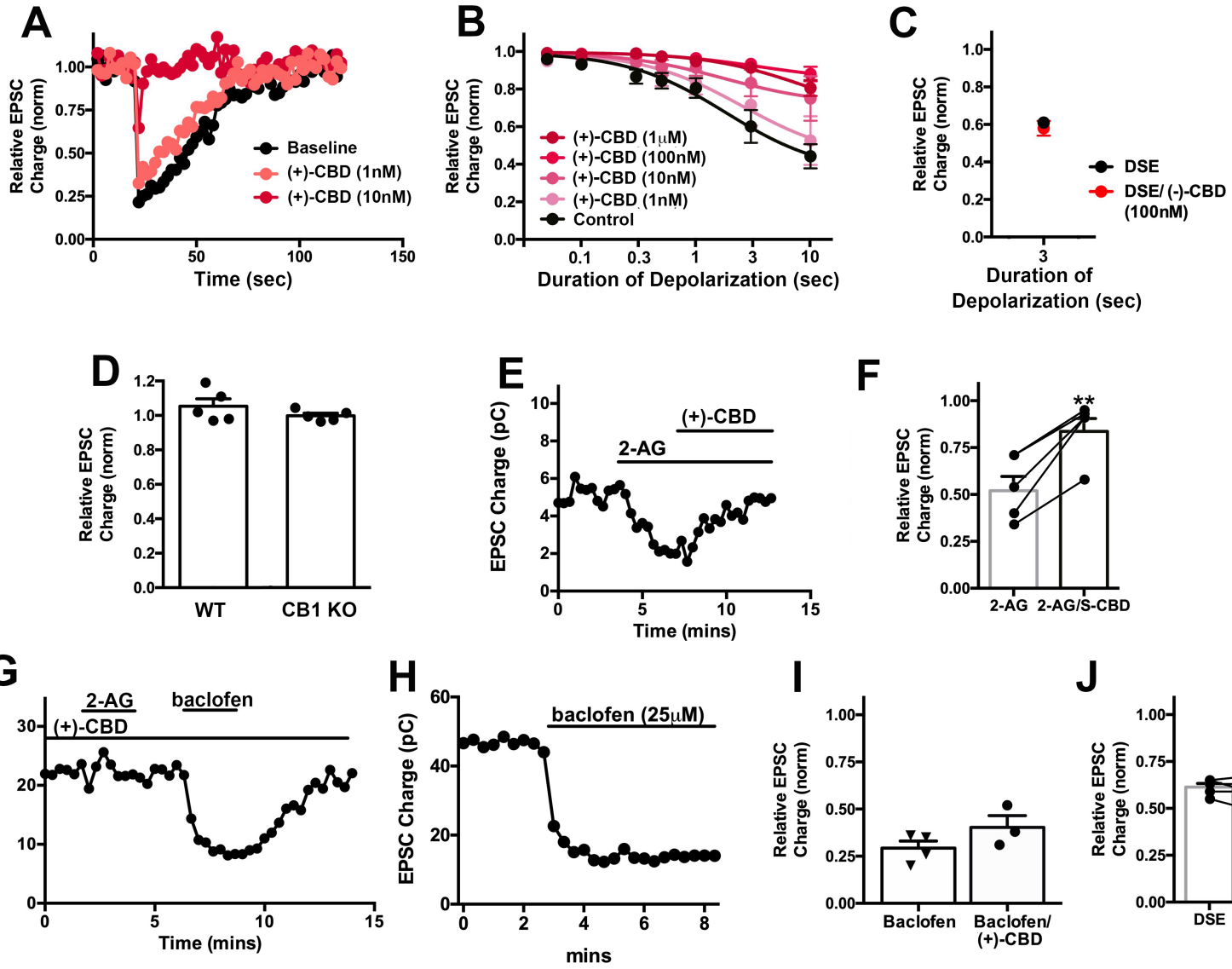

Figure 3

Molecular Pharmacology Fast Forward. Published on September 24, 2022 as DOI: 10.1124/molpharm.121.000305
This article has not been copyedited and formatted. The final version may differ from this version.

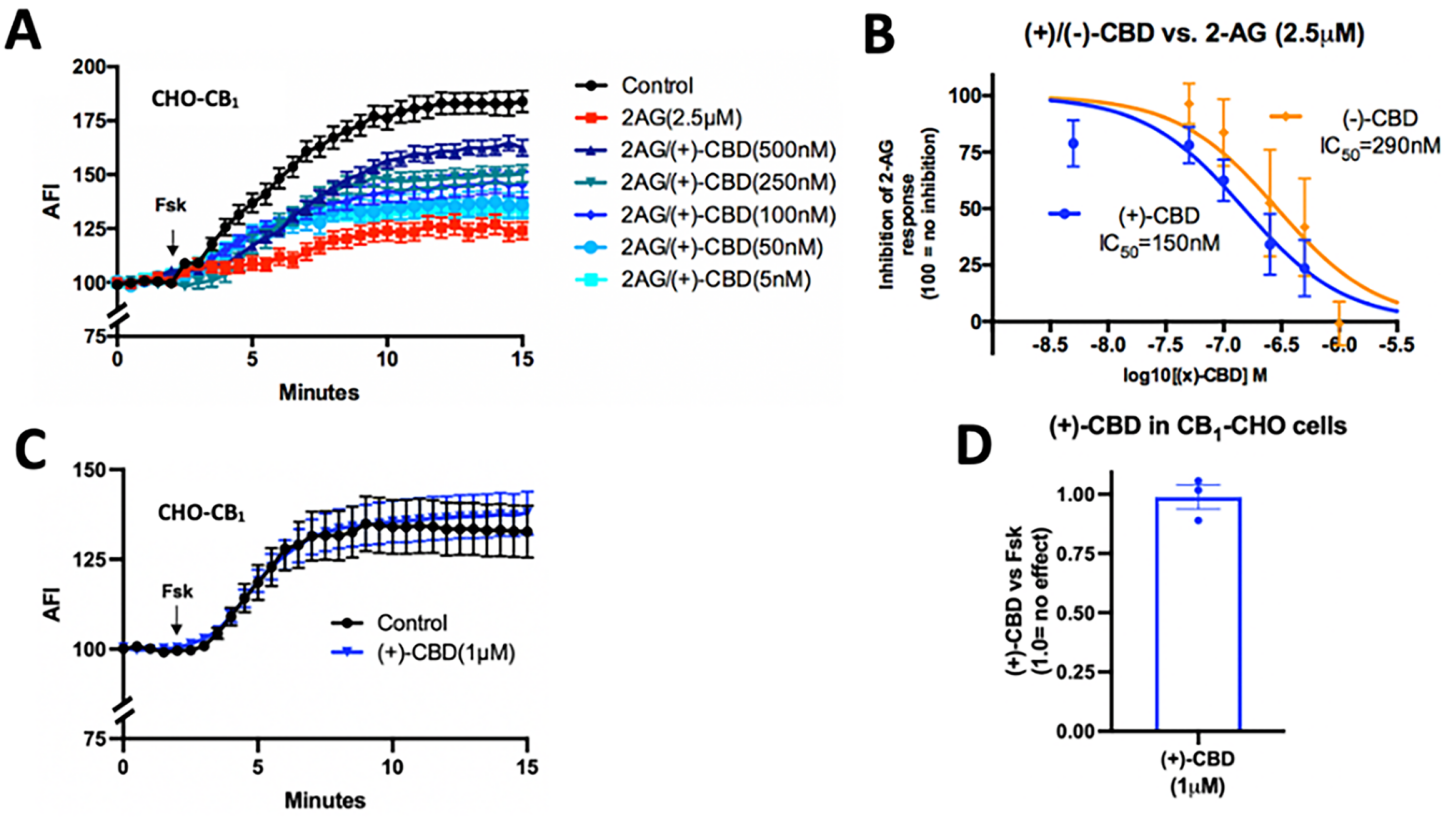

Figure 4

Molecular Pharmacology Fast Forward. Published on September 24, 2022 as DOI: 10.1124/molpharm.121.000305
This article has not been copyedited and formatted. The final version may differ from this version.

Figure 5.